Journal of Hydrology 566 (2018) 285–298

Contents lists available at ScienceDirect

Journal of Hydrology

journal homepage: www.elsevier.com/locate/jhydrol

Research papers

The impact of climate change on inland waterway transport: Effects of low water levels on the Mackenzie River

H. Scheepers, J. Wang, T.Y. Gan*, C.C. Kuo

Department of Civil & Environmental Engineering, University of Alberta, Canada

ARTICLE INFO

This manuscript was handled by marco borga, Editor-in-Chief, with the assistance of Ashish Sharma, Associate Editor

Keywords:
Mackenzie River Basin
Water level
Arctic transportation network
Impacts of Climate Change
Statistical downscaling
HBV hydrologic model

ABSTRACT

Potential impact of climate change on the inland waterway transport of the Mackenzie River Basin (MRB) have been investigated through simulations of the Hydrologiske Byrån avdeling för Vattenbalans (HBV) hydrological model, the HBV-light, for the baseline, 1974–2004, and future periods of 2041–2070 and 2071–2100 over the MRB driven by precipitation and air temperature data of Representative Concentration Pathways, RCP4.5 and RCP8.5 climate scenarios of 10 Global Climate Models statistically downscaled by the Pacific Climate Impacts Consortium using the Bias-Correction Spatial Disaggregation. The average onset of spring snowmelt between 2041 and 2100 is projected to occur up to two weeks earlier than the historical (1974–2004) climate. Projected warmer temperature and higher precipitation will lead to higher runoff for MRB in winter and spring, at the expense of decreased summer streamflow and water level at Fort Simpson and Arctic Red River stations partly because projected increase in evapotranspiration will offset the projected increase in precipitation. Under a warmer climate, navigation issues related to low water levels are expected to increase, e.g., under RCP8.5 at Arctic Red River station, the number of days the water level above 5 m is projected to decrease from 74 days in 1974–2000 to 42 days in the 2080s. The summer durations that water levels of MRB will be at or above 3, 4, and 5 m are projected to decrease by 2.8%–22.2%, 10.0%–34.5%, and 16.2%–43.4%, respectively, which mean navigation problems would increase because safe transit through MRB depends on its water levels.

1. Introduction

Climate change has affected river basins worldwide, both socially and environmentally, including the Mackenzie River Basin (MRB) of Canada. The water resources of MRB are of key interest to Canada, and the Mackenzie River provides the largest source of freshwater from North America to the Arctic Ocean. In addition, the stage of the Mackenzie River plays a major role to the transportation of northern communities of Northwest Territories (NWT), e.g., the Mackenzie River provides a critical corridor in Canada's Arctic transportation network. During the relatively short open water season of May to October, the Mackenzie River carries barge traffic for supply and bulk fuel shipments to the north (Arctic Council, 2009). The Mackenzie River is a major river of the world, ranks 10th by length and 13th by drainage area. It provides an active transportation corridor for residents, because most residents living along the river travel by snowmobile on the ice cover in winter and by personal watercraft in the summer. In other words, the water levels of the Mackenzie River play a major role to the transportation of the northern communities of NWT.

Modern transportation is essential for our society to function, but as an economic sector, it is the fourth largest contributor to global greenhouse gases (GHG) emissions (IPCC, 2014). Climate warming has caused extreme climate to occur more frequently worldwide, including the MRB (Trenberth et al., 2003). This study focuses on potential effects of climate change on the water level of the Mackenzie River, a major inland waterway transport of Canada's north, which is likely more sensitive to climate change impact than other modes of transport of northern Canada.

Inland waterway transport generally has a low environmental impact compared to transportation involving heavy vehicles (McKinnon, 2007). To investigate the hydrologic impact of climate change to MRB, Sung et al. (2006) simulated the future streamflow of MRB by forcing a physics-based distributed hydrologic model, WATFLOOD of Kouwen et al. (1993) with climate change scenarios of three Global Climate Models (GCMs). They then routed the simulated streamflow using the hydraulic routing model River 1D Model of Hicks and Steffler (1992). Under a warmer climate projected by IPCC (2013), an earlier spring freshet and a lower streamflow in the summer but higher in the fall could extend the navigation season of MRB to about 137 days. However, given the carrying capacity of the inland water transport of MRB

* Corresponding author.
E-mail address: tgan@ualberta.ca (T.Y. Gan).

https://doi.org/10.1016/j.jhydrol.2018.08.059
Received 24 April 2018; Received in revised form 21 August 2018; Accepted 27 August 2018
Available online 12 September 2018
0022-1694/ © 2018 Elsevier B.V. All rights reserved.

also depends on its water level, lower summer water levels in the future could offset the benefit of an extended navigation season due to climate change impact (Zheng and Kim, 2017).

According to the Canadian Mackenzie GEWEX Study (MAGS) (Stewart et al., 1998), a major contributor to the Global Energy and Water cycle Exchanges (GEWEX) project which focuses on atmospheric and the hydrologic systems of MRB, MRB has experienced a pronounced warming trend, which could be up to 2 °C per decade in some locations during winters (Cohen, 1997). For example, the annual temperature in Inuvik near the Arctic Ocean has increased by about 3 °C since the 1940s (Environment and Natural Resources, GNWT, 2008). In recent decades, a warmer climate had resulted in various climatic and environmental changes, such as more intensive storms, more severe droughts, less soil moisture, shorter winter ice seasons, significant thinning of sea ice and freshwater ice, reduction in snow cover, thawing of permafrost, glaciers, and ice sheets, earlier onset and larger volume of spring melt runoff, and increased coastal erosion of shorelines (Huntington and Fox, 2005; Gan et al., 2016; Gobena and Gan, 2013; Weller et al., 2005; Barry and Gan 2011; Kuo et al., 2015). Each year, between May-October, the Mackenzie River provides the bulk transportation to northern communities of NWT. However, it was shut down about a month earlier in 2015 because of low water levels. The Northern Transportation Company battled even lower water levels with lighter loads and more barges in the second straight season of 2016. The reduced discharge and low water levels has limited the cargo-carrying capacity of vessels and increased the shipping costs to the north in recent years.

Climate change impacts could lead to greater uncertainties in future streamflow and water levels of the Mackenzie (Kerr, 1997). Based on composite climate scenarios for the MRB, Soulis et al. (1994) and Kerr (1997) found that the precipitation of MRB was projected to increase, which should have resulted in a higher runoff, but enhanced evapotranspiration has led to lower streamflow and lake levels in the MRB. They also projected that the spring ice break-up will occur earlier with higher spring snowmelt runoff under climate change impact.

The main objective of this study is to investigate how the possible hydrologic impact of climate change on MRB will contribute to physical limitations of the critical corridor of Canada's Arctic transportation network. The potential climate change impact on water levels of the Mackenzie River, a crucial factor for the inland waterway transport, was simulated by the conceptual hydrologic model HBV-light (Hydrologiske Byrån avdeling för Vattenbalans-light) (Seibert and Vis, 2012) driven by statistically downscaled climate scenarios of ten GCMs (Table 1) of the Pacific Climate Impacts Consortium (PCIC). Compared to Sung et al. (2006), this study estimated uncertainties associated with long-term climate projections of MRB by using more and newer climate scenarios of the Intergovernmental Panel on Climate Change (IPCC) of 2013 statistically downscaled by PCIC. The results of this study will be useful for planning the inland water transport of MRB, and its future municipal infrastructure development to mitigate the potential impact of climate change. With the above introduction, the study site, data, and research methodology are given in Section 2, discussion of results in Section 3 and conclusions in Section 4.

2. Study site, data and methodology

2.1. Study site – Mackenzie River basin (MRB)

As the largest river basin of Canada, MRB can be divided into five main sub-basins (Table 2), three great lakes, and three major deltas. The main headwaters are the Columbia Ice field in the Jasper National Park and snowfields of the upper Peace River in northeastern British Columbia. With a huge land area of about 1.8 million km^2, MRB lies between 51°N to almost 70°N, experiences mild summers and cold winters in the south to long cold winters and short cool summers in the north (Stewart et al., 1998). Further, MRB is currently experiencing a warming trend (Environment and Natural Resources, GNWT, 2008). MRB receives a mean annual precipitation of 410 mm with 6 to 8 months of snowfall. Its mean temperatures are about −25 °C to −30 °C in winter and 15 °C in summer. The annual mean evapotranspiration is about 230 mm, which mainly occurs between May and October. The annual mean discharge of the Mackenzie River into the Arctic Ocean is about 9100 m^3/s, or approximately 180 mm per year of runoff.

There are six major rivers within the MRB (Fig. 1 and Table 3). The Athabasca River is the upstream river and is located in the most southern area of the MRB. The confluence of the Athabasca River and the Peace River with Lake Athabasca forms the Peace-Athabasca delta. The W.A.C. Bennet Dam is located at the head of the Peace River and has had regulated streamflow since 1967. The demands of electric power production resulted in greater winter flows in the Peace River, while the spring and summer peaks have been suppressed (Seneka, 2004). The Peace River flows into the Slave River, which enters the Great Slave Lake, the fifth largest lake in North America. The Mackenzie River starts at the extreme west end of the Great Slave Lake and empties into the Beaufort Sea through the Mackenzie Delta. The majority of the

Table 1
Details of the PCIC's BCSD statistically downscaled RCP climate scenarios of IPCC (2013).

No.	RCP	Ensemble	Model Designation	Climate Modelling Group	Group Acronym	Country
1	4.5	r1i1p1	ACCESS 1–0	Commonwealth Scientific and Industrial ResearchOrganisation (CSIRO) and Bureau of Meteorology (BOM)	CSIRO- BOM	Australia
2	8.5					
3	4.5	r1i1p1	CanESM2	Canadian Centre for Climate Modelling and Analysis	CCCMA	Canada
4	8.5					
5	4.5	r2i1p1	CCSM4	National Centre for Atmospheric Research	NCAR	USA
6	8.5					
7	4.5	r1i1p1	CNRM-CM5	Centre National de Recherches Météorogiques/ Centre Européen de Recherche etFormation Avanceé en Calcul Scientifique	CNRM-CERFACS	France
8	8.5					
9	4.5	r1i1p1	CSIRO-Mk3-6–0	Commonwealth Scientific and Industrial ResearchOrganisation in collaboration with the Queensland Climate Change Centre of Excellence	CSIRO- QCCCE	Australia
10	8.5					
11	4.5	r1i1p1	GFDL-ESM2G	NOAA Geophysical Fluid Dynamics Laboratory	NOAA GFDL	USA
12	8.5					
13	4.5	r1i1p1	inmcm4	Institute for Numerical Mathematics	INM	Russia
14	8.5					
15	4.5	r3i1p1	MIROC5	Japan Agency for Marine-Earth Science and Technology, Atmosphere and Ocean Research Institute (TheUniversity of Tokyo), and National Institute for Environmental Studies	MIROC	Japan
16	8.5					
17	4.5	r3i1p1	MPI-ESM_LR	Max-Planck Institute für Meteorologie (Max Planck Institute for Meteorology)	MPI-M	Germany
18	8.5					
19	4.5	r1i1p1	MRI-CGCM3	Meteorological Institute	MRI	Japan
20	8.5					

Table 2
Characteristics of the Mackenzie River Basin divided into five sub-basins.

Sub-basin Number	1	2	3	4	5
Hydrometric station	Peace River at Peace River	Athabasca River at Athabasca	Liard River Near the Mouth	Mackenzie River at Fort Simpson	Mackenzie River at Arctic Red River
Station ID	07HA001	07BE001	10ED002	10GC001	10LC014
Latitude (°N)	56.2°N	54.7°N	61.7°N	61.9°N	67.5°N
Longitude (°W)	117.3°W	113.3°W	121.2°W	121.4°W	133.7°W
Drainage Area (km^2)	194 374.2	74 602.3	275 000	1 301 435	1 679 100
Period of Continuous Streamflow Record	1/1/1969 – 31/12/2007	1/5/1951 – 31/12/2013	27/5/1972 – 31/12/2013	1/1/1965 – 31/12/2013	15/8/1972 – 31/10/19971/4/1998 – 31/12/2013

Mackenzie River is situated within the Great Bear Lake basin, which starts at Fort Simpson where the Liard River reaches the Mackenzie River. The Mackenzie Delta commences at a location called the Point Separation from which the Mackenzie River splits into three major channels: the east Channel, the Middle Channel, and the Peel Channel. Streamflow entering the Mackenzie Delta is typically measured where the Arctic Red River enters the Mackenzie River, approximately 25 km upstream of Point Separation. In this study, the streamflow of the Athabasca and Peace River basins have been separately simulated by HBV, and compared with the long-term observed streamflow data of the gauging stations of Fort Simpson and Arctic Red River, respectively (Fig. 1).

2.2. Data

Water levels of the Mackenzie River were analyzed over the historical baseline of 1974–2004 and the projected period of 2041–2100. Daily 10-km gridded precipitation and temperature data are taken from the ANUSPLIN (Australian National University SPLINe) dataset of Environment Canada (Hutchinson et al., 2009). The mean daily temperature was calculated as the average of the minimum and maximum temperature time series. The HBV model was also calibrated using data from 31 climate stations available in the Second Generation of Daily Adjusted Precipitation (Mekis and Vincent, 2011) and the Second Generation of Homogenized Temperature dataset for Canada (Vincent et al., 2012). HBV was configured by using both the gridded and areally weighted climate station data as input, which yielded comparable results. However, HBV driven by climate station data required an additional parameter to adjust its temperature and precipitation with elevation. Such a model configuration was not compatible with gridded data from climate change scenarios, and therefore only the model configuration and results using ANUSPLIN data are discussed here.

Digital Elevation Map (DEM) data of the Mackenzie of 3 arc-seconds (35–93 m) resolution were used to characterize the terrains of the five sub-basins of MRB using elevation bands at 200 m intervals. The land use information for MRB was obtained from MODIS (Moderate Resolution Imaging Spectroradiometer) Terra + Aqua Land Cover Type Yearly L3 Global 500 m SIN Grid product (PLP DAAC, 2012). MODIS is a sensor mounted on the Terra and Aqua satellite. The dataset consist of

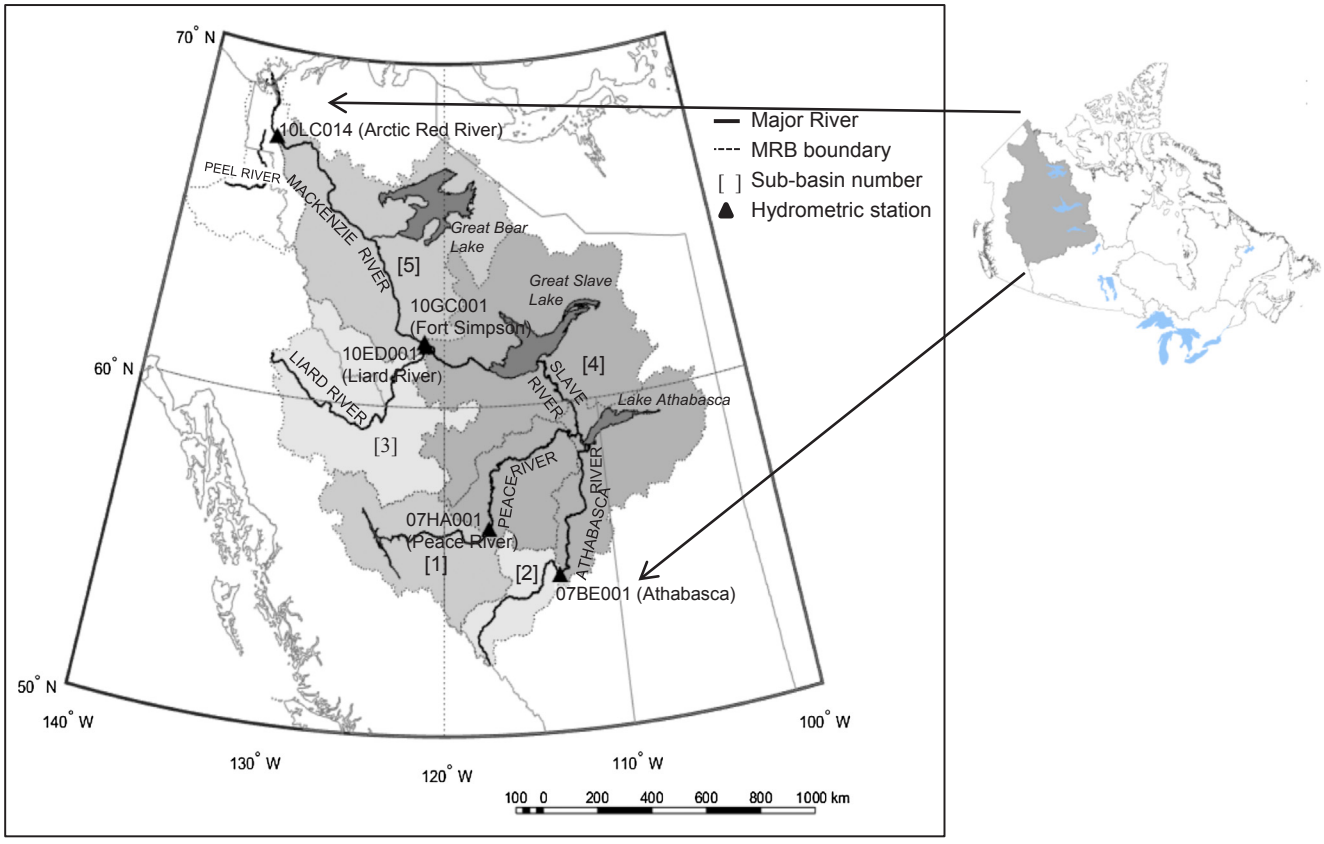

Fig. 1. The Mackenzie River Basin (MRB) of Canada and the sub-basins used in the HBV model.

Table 3
Characteristics of seven gaging stations of the Mackenzie River Basin.

	River Sub-basin						
Sub-basin Number	1	2	3	4	5	6	7
Discharge gauging station	Peace River at Peace River	Peace River at Peace Point	Athabasca River at Athabasca	Slave River at Fitzgerald	Liard River Near the Mouth	Mackenzie River at Fort Simpson	Mackenzie River at Arctic Red River
Station ID	07HA001	07KC001	07BE001	07NB001	10ED002	10GC001	10LC014
Latitude	56.2°N	59.1°N	54.7°N	59.9°N	61.7°N	61.9°N	67.5°N
Longitude	117.3°W	112.4°W	113.3°W	111.6°W	121.2°W	121.4°W	133.7°W
Drainage area (km^2)	194 374.2	293 000	74 602.3	606 000	275 000	1 301 435	1 679 100
Period of Continuous Streamflow Record	1/1/1969 – 31/12/2007	1/1/1969 – 31/12/2007	1/5/1951 – 31/12/2013	1/5/1959 – 7/5/2011	27/5/1972 – 31/12/2013	1/1/1965 – 31/12/2013	15/8/1972 – 31/10/19971/4/1998 – 31/12/2013

land cover classes developed from one year of remotely sensed data acquired by the Terra- and Aqua-MODIS sensor. There are five different classification schemes in this product. In this study, the Land Cover Type 5: Plant Functional Type (PFT) scheme which contained 12 different land cover types was chosen and reclassified to three land cover types because HBV model parameters could be specified for up to three land cover types.

Historic daily snow water equivalent (SWE) data between 1 November 1988 and 31 March 2016 for MRB was extracted from the GlobSnow dataset. It contains SWE estimate for the whole Northern Hemisphere, between latitudes 35° and 85° excluding mountainous regions and Greenland with a nominal spatial resolution of 25 km. Takala et al. (2011) provide a full description of the methodology for the Globsnow SWE estimates. Within the MRB, there were 2294 grids with SWE data, excluding water and mountainous regions. The Mann-Kendall test (Kendall, 1948; Mann, 1945) was used to estimate trends that were significant at the 0.05 level. Trend magnitude in mm/yr was estimated using the Theil-Sen approach (Theil, 1950; Sen, 1968).

This study used daily precipitation, minimum and maximum temperature data of Canada for climate change scenarios of ten GCMs of CMIP5 (IPCC, 2013) statistically downscaled by the PCIC (Pacific Climate Impacts Consortium) (Table 1). PCIC statistically downscaled the output of twelve Global Climate Models (GCMs) of IPCC (2013) of 1950 to 2100 at a resolution of 300 arc-seconds, which is approximately 10-km. The statistical downscaling was performed using the Bias Corrected Spatial Disaggregation (BCSD) technique (Werner, 2011) and the Bias Correction/Constructed Analogues with Quantile mapping reordering (BCCAQ) technique (Werner and Cannon, 2015). Comparing the BCSD and BCCAQ method data with the CanESM2 model, the BCSD method resulted in an average temperature distribution that was more in line with average historical observations over the same period. Therefore, the BCSD data was selected for all subsequent GCMs. A systematic description of the BCSD method can be found in Werner (2011), who also summarized it in three steps: a) Use quantile mapping to perform bias correction of the GCM fields. b) Apply "local scaling" of the corrected fields to the target higher resolution of the application and c) use the monthly averages of the locally scaled fields to re-sample the daily historic record. The BCSD method described by Wood et al. (2004) and Maurer and Hidalgo (2008) was modified and adjusted. The modifications used by the PCIC include incorporating monthly minimum and maximum temperatures instead of monthly mean temperatures, and bias correction using detrended quantile mapping with the delta method extrapolation. According to Werner (2011), the BCSD method is advantageous in its ability to capture trends in the regional climate and hydrologic response as well as the transient nature of the emissions scenarios. A disadvantage is that if the output data from a GCM is poor, the same limitations are carried forward in the downscaling process.

The PCIC downscaled datasets are based on GCMs' projections for three Representative Concentrated Pathways (RCP), but only RCP4.5 and 8.5 scenarios were considered in this study. Radiative forcing in RCP4.5 peaks at about 4.5 W/m^2 (~540 ppm CO_2) in year 2100. RCP4.5 is comparable to the SRES (Special Report Emission Scenario) scenario B1 with similar CO_2 concentrations and median temperature increases by 2100. RCP8.5 assumes a high rate of radiative forcing increase, peaking at 8.5 W/m^2 (~940 ppm CO_2) in year 2100. RCP8.5 assumes higher CO_2 concentrations than SRES A2 scenarios by 2100 (IPCC, 2007, IPCC, 2013).

Streamflow of MRB was modelled by calibrating HBV against streamflow of five hydrometric stations separately, starting first from sub-basin #1, then sub-basin #2, until sub-basin #5. The division of the sub-basins were based on the quality of available streamflow data taken from the Water Survey Canada's hydrometric database (HYDAT) of Environment Canada (2013). Naturalized streamflow for station 07HA001 on the Peace River was obtained from the Government of Alberta (Seneka, 2004). Hydrometric stations downstream of the Peace River with records that were likely significantly influenced by regulated flows were excluded. The final hydrometric stations used in this study are given in Fig. 1 and Table 2.

Stage-discharge tables for Fort Simpson and Arctic Red River stations on the Mackenzie River were obtained from the Water Survey of Canada. Best-fit nonlinear regression equations were developed from the stage-discharge data and applied to convert simulated discharge values to river stages in meters.

3. Research methodology

To study the possible impact of climate change on the inland waterway transport of the Mackenzie River, the Hydrologiske Byrån avdeling för Vattenbalans (HBV) model (Bergstrom, 1975) was selected to simulate the hydrological response of MRB. HBV was originally developed at the Swedish Meteorological and Hydrological Institute (SMHI) for runoff simulation and hydrological forecasting in the early 1970s. As a conceptual, semi-distributed, rainfall-runoff model for modeling catchment hydrology, HBV has been used to perform various impact studies for climate change assessments (Kuo et al., 2017; Bergstrom et al., 2001; Vehviläinen and Huttunen, 1997). This study used the latest version of HBV, the HBV-light model of Seibert and Vis (2012) which is set up with three conceptual storage tanks as soil moisture zone, upper and lower zones, respectively. It operates with daily precipitation, temperature, and evaporation as input data.

4. The HBV-light model

The HBV-light model consists of routines for modeling snow accumulation and snowmelt, soil moisture accounting, a runoff response function, and a runoff routing procedure (Fig. 2). As a semi-distributed hydrologic model, HBV considers spatial climate variabilities by modeling each sub-basin with different temperature, precipitation, and evaporation time series. Given significant climatic and hydrologic variabilities have been observed in Canada (Mwale et al., 2009), which could be linked to climate anomalies (Jiang et al., 2014), this is an effort to account for uncertainties associated with catchment hydrologic

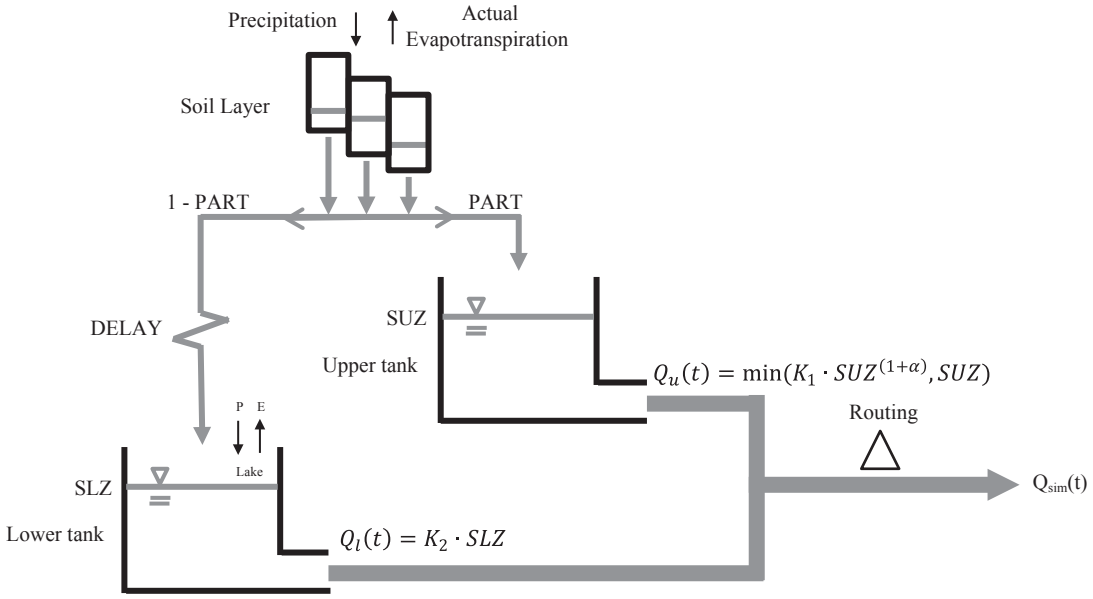

Fig. 2. Model structure of the HBV model (modified from HBV Help Manual).

modeling. Since each sub-basin may have more than one climate stations, areally weighted mean daily temperature and precipitation for each sub-basin were calculated using the Thiessen polygon method. Potential evapotranspiration (*PET*) was estimated from air temperature using Hamon's (1961) temperature-index equation (Eq. (1).

$$PET = \frac{29.8 \times D \times e_s}{T + 273.3} \quad (1)$$

where $e_s = 0.611 \times e^{\frac{17.27T}{T+237.3}}$ is the saturation vapor pressure (*kPa*), *PET* in *mm/day*, *D (hrs)* the daylight hours, and *T* (^oC) the mean daily temperature.

The snow routine accounts for snow accumulation and snowmelt by a simple degree-day approach while the soil moisture routine estimates groundwater recharge and actual evaporation as a function of the water storage. Excessive water from precipitation and snowmelt is transformed to runoff by a response function. It consists of two conceptual storages (tanks) that simultaneously re-distribute the generated runoff as quick and slow responses, respectively. The recharge from the soil routine is divided into two parts. The portion of the recharge added to the upper tank is computed using the parameter *PART*. The upper tank runoff, the basin's quick runoff responses $Q_u(t)$, is assumed to be the lesser value of the upper tank storage, *SUZ (mm)* and $K_1 \cdot SUZ^{(1+\alpha)}$ *(mm)*, where α is a non-linearity coefficient and K_1 *(day^{-1})* is a recession coefficient:

$$Q_u(t) = \min(K_1 \bullet SUZ^{(1+\alpha)}, SUZ) \quad (2)$$

The remaining discharge generated in one day is distributed evenly over the subsequent period defined by the *DELAY (day)* parameter. The product of the lower tank storage *SLZ (mm),* and the recession coefficient K_2 *(day^{-1})* is the lower tank runoff, $Q_l(t)$ given as

$$Q_l(t) = K_2 \bullet SLZ \quad (3)$$

In the routing routine, the runoff to the catchment outlet is simulated using an equilateral triangular weighting function of length *MAXBAS*. The runoff from both tanks $Q_{ul}(t) = Q_u(t) + Q_l(t)$ is further transformed by:

$$Q_{sim}(t) = \sum_{i=1}^{MAXBAS} c(i) \bullet Q_{ul}(t-i+1) \quad (4)$$

where $c(i) = \int_{i-1}^{i} \frac{2}{MAXBAS} - \left| u - \frac{MAXBAS}{2} \right| \bullet \frac{4}{MAXBAS^2} du$

Model parameters, *TT* (threshold temperature for precipitation), *CFMAX* (degree-day melt coefficient), *SFCF* (snowfall correction factor), *FC* (maximum soil moisture storage), *LP* (soil moisture value above which *AET* reaches *PET*), β (parameter that determines the relative contribution to runoff from rain or snowmelt), α, recession cofficients K_1 and K_2, *MAXBAS*, *PART* (portion of the recharge added to groundwater box 1), and *DELAY* (time period over which recharge is evenly distributed) as well as height increment variables *PCALT*, *TCALT*, *Pelev*, and *Telev*, when applicable, are calibrated using a Monte Carlo calibration tool built inside the HBV-light model. The other two HBV model parameters, *CFR* (refreezing coefficient) and *CWH* (water holding capacity) are set at 0.05 and 0.1, respectively as recommended, instead of being calibrated.

The basin was also divided into different elevation bands. For each elevation band, the temperature and precipitation was adjusted with respect to its elevation above sea level by the parameter *TCALT (%/100 m),* the lapse rate with the elevation, *Telev (m),* of temperature data, and *PCALT (%/100 m),* the change of precipitation with elevation, *Pelev (m),* of precipitation data.

HBV was calibrated against the observed streamflow data using ANUSPLIN data as input over the period 1/1/1974–31/12/1997 by the Monte Carlo approach and GAP (Genetic Algorithm & Powell's quadratically convergent method) (Seibert, 2000; Press et al., 2002) for each of the five sub-basins separately. The first year data of 1973 was used as spin-up for HBV in order to establish proper initial conditions for the calibration and validation periods and therefore was not included in the results. The Monte Carlo procedure performs a large number of simulations, and each individual simulation is allocated random parameter values from pre-defined parameter ranges. This resulted in five sets of optimized HBV parameters, one set for each of the five sub-basins of MRB. Observed streamflow of Mackenzie at Station 10GC001 of Fort Simpson was the upstream site chosen in the calibration. Because HBV is not set up to model the Mackenzie Delta, which is a wetland, the downstream station, selected for the Mackenzie River was Station 10LC014 of the Arctic Red River.

HBV was automatically calibrated using an objective function based on the Nash-Sutcliffe (*NS*) coefficient (Nash and Sutcliffe, 1970) (Eq. (5) that minimizes differences between the simulated streamflow of HBV versus the observed.

$$NS = 1 - \frac{\sum_{t=1}^{n} (Q_{Obs}(t) - Q_{Sim}(t))^2}{\sum_{t=1}^{n} (Q_{Obs}(t) - \bar{Q}_{Obs})^2} \quad (5)$$

where $\bar{Q}_{Obs}$ is the mean observed streamflow, $Q_{Obs}(t)$ $Q_{Sim}(t)$ the

Table 4
Goodness-of-fit statistics, coefficient of determination (R2), Nash-Sutcliffe coefficient (NS) and Root Mean Square Error (RMSE) for the calibration and validation of hydrometric stations of Mackenzie River.

Hydrometric Station	Calibration			Validation		
	R^2	NS	RMSE (mm/day)	R^2	NS	RMSE (mm/day)
Peace River at Peace River (07HA001)	0.79	0.79	0.41	0.81	0.81	0.38
Athabasca River at Athabasca (07BE001)	0.82	0.82	0.21	0.81	0.78	0.19
Liard River Near the Mouth (10ED002)	0.83	0.83	0.33	0.86	0.86	0.27
Mackenzie River at Fort Simpson (10GC001)	0.86	0.84	0.12	0.84	0.83	0.11
Mackenzie River at Arctic Red River (10LC014)	0.88	0.88	0.12	0.87	0.86	0.12

simulated streamflow, and *n* the total number of time steps. HBV is well calibrated with physically meaningful parameters if the *NS* obtained in both the calibration and validation stages are close to 1. The calibrated model was validated against observed streamflow data for the period 1/1/1998-31/12/2004 independent of the calibration experience.

ANUSPLIN, likely is the best gridded dataset available for Canada, was used to calibrate HBV for MRB over the baseline period. After the calibrated HBV was validated, it was forced with precipitation and air temperature data downscaled by PCIC using the BCSD statistical downscaling method (Werner and Cannon, 2016) for RCP4.5 and RCP8.5 climate change scenarios of 10 GCMs of IPCC (2013) to simulate an ensemble of hydrologic responses of MRB to climate change impact over 2050s (2041–2070) and 2080s (2071–2100), respectively. By considering climate scenarios of many GCMs of CMIP5, we can estimate uncertainties associated with hydrologic responses of MRB to long-term climate projections.

Water levels of rivers can be estimated using a hydraulic model based on observed streamflow data and detailed river cross-section information. Because of a lack of measurement on the cross-section of the Mackenzie River, best-fit nonlinear regression equations developed from the stage-discharge data were applied to convert simulated future discharge to future river stages of the Mackenzie in meters.

5. Discussion of results

Results were obtained for all five sub-basins. However in this section results are for the most part presented and discussed for the Fort Simpson and Arctic Red River stations located on the Mackenzie River only, because this is the focus of the study. Even though these two stations do not represent the Mackenzie River as a whole, they represent the general upstream and downstream conditions of MRB, respectively.

5.1. Calibration and validation of HBV

At the calibration (validation) stage, the coefficient of determination, R^2, and the Nash-Sutcliffe coefficient, NS, obtained for the calibration and validation periods for HBV ranged between 0.78 and 0.88 as shown in Table 4. For the Mackenzie River, R^2 and NS coefficient obtained for the calibration period are 0.86 and 0.84 at Fort Simpson and 0.88 for both statistics at Arctic Red River, respectively. The validation runs resulted in a R^2 of 0.84 and NS of 0.83 at Fort Simpson, and a R^2 of 0.87 and NS of 0.86 at Arctic Red River. Selected streamflow hydrographs simulated by HBV during the validation stage for Fort Simpson and Arctic Red River are shown in Fig. 3. HBV accurately simulated the spring snowmelt, which has a sharp peak compared to the winter flow, but it marginally under-simulated the falling limb of the hydrograph. The simulated base flow in the winter is under-simulated compared to the observed flow. This could in part due to inaccurate measurements of the ice-covered river in winter, and in part due to the flow regulation of the W.A.C. Bennet Dam, instead of under simulation of snowmelt, which in MRB should be minimal during winter (Singh et al., 2009). Thus, for both Fort Simpson and Arctic Red River stations, HBV forced with the ANUSPLIN dataset can simulate the streamflow of

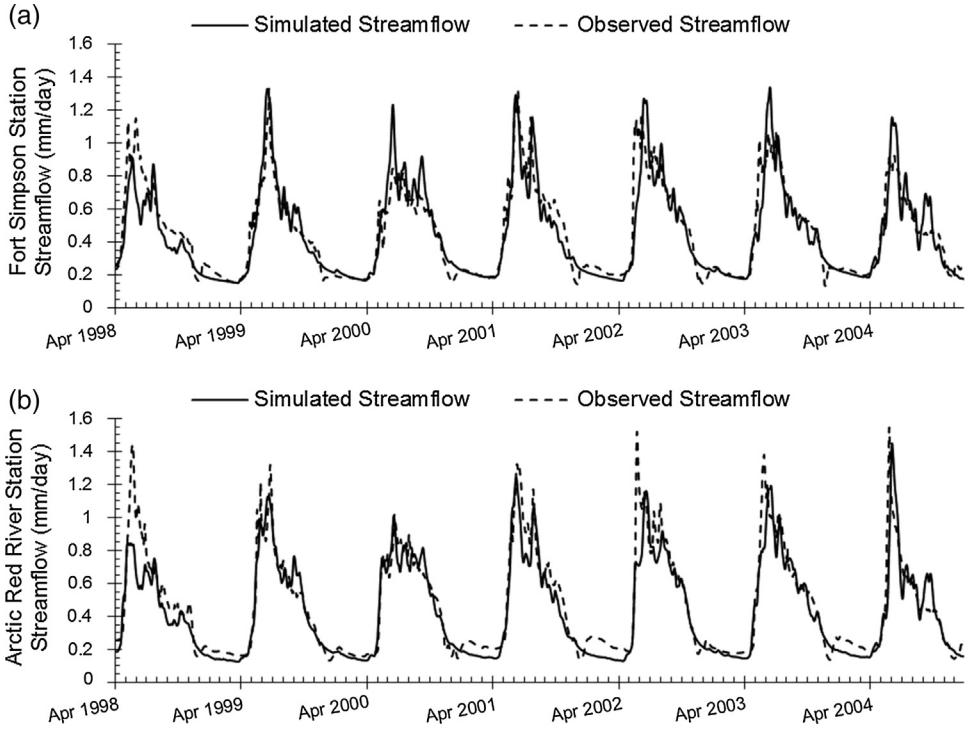

Fig. 3. Observed versus streamflow simulated by HBV driven by ANUSPLIN data at a) the Fort Simpson station (10GC001), b) the Arctic Red River station (10LC014) of the Mackenzie River over the validation period of 1998–2004.

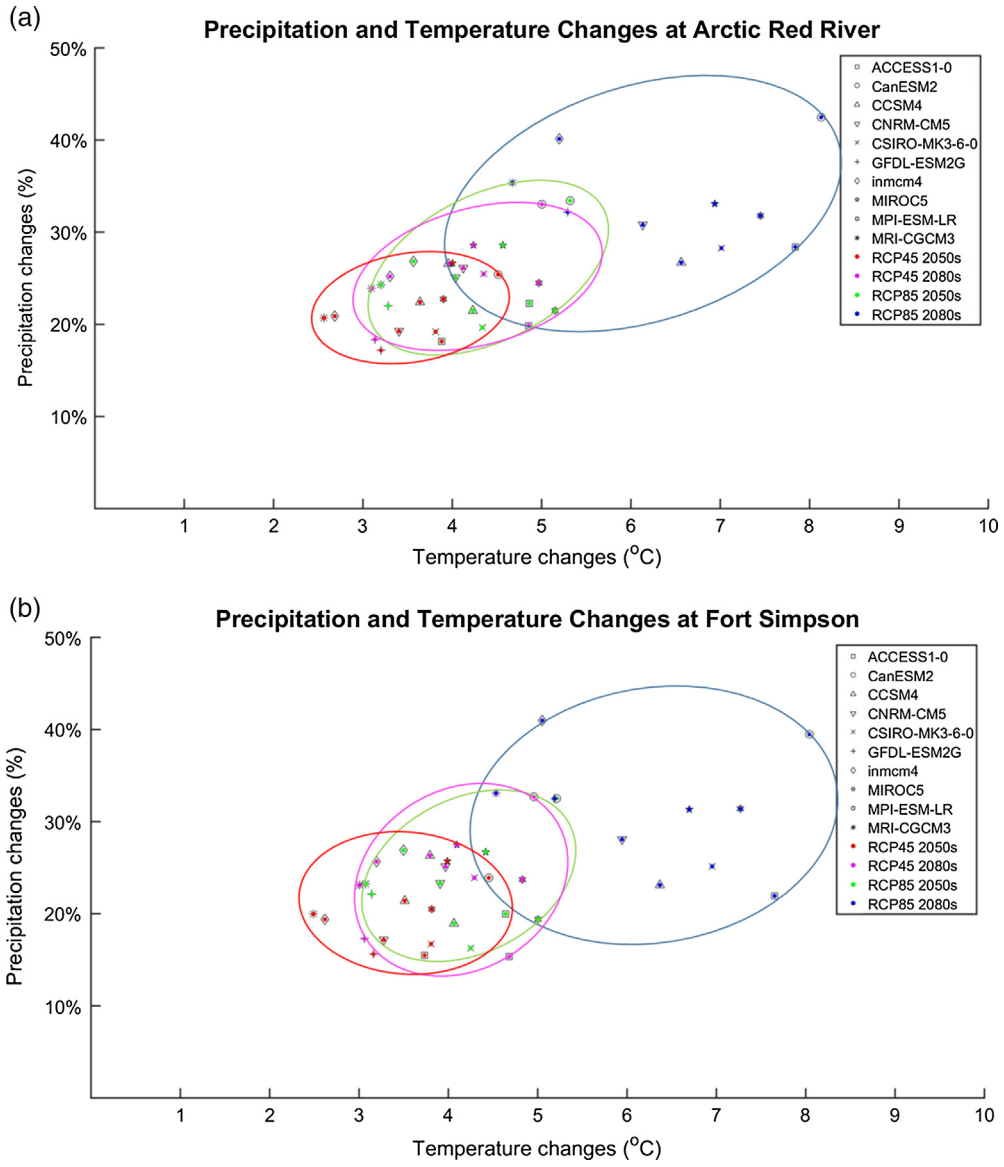

Fig. 4. Projected change in precipitation (%) and Temperature (°C) for climate scenarios of 2050s and 2080s for ten GCMs of IPCC (2013) at Fort Simpson and Arctic Red River stations, respectively, where ellipses encompass all projected changes, ΔT and ΔP, under RCP4.5, RCP8.5 for 2050s and 2080s, to the areas upstream of (a) Arctic Red and (b) Fort Simpson. (For interpretation of the references to colour in this figure legend, the reader is referred to the web version of this article.)

MRB that agree closely with the hydrometric measurements. This means that HBV is well calibrated, its optimized model parameters are physically meaningful, and therefore there is sufficient basis to use the calibrated HBV to simulate the impact of climate change to MRB, assuming MRB will be subjected to minimal landuse change and other possible human impacts in the future.

After HBV was calibrated and validated with the ANUSPLIN data, driving HBV with PCIC's statistically downscaled data for the base period generally resulted in over-simulated streamflow compared to streamflow simulated using the ANUSPLIN data and observed streamflow, even though the over-simulation problem varies from GCM to GCM. Therefore, the precipitation of each GCM for MRB was individually reduced by a constant factor across the entire MRB so that the mean simulated streamflow of HBV driven by the GCMs' precipitation data for the base period agree well with the observed historic streamflow data. The precipitation adjustment factors varied between 10% and 13% for different GCMs.

5.2. Changes of precipitation and air temperature

Projected changes of PCIC's statistically downscaled precipitation and air temperature data under RCP4.5 and RCP8.5 climate change scenarios of 10 GCMs of IPCC (2013) over 2050s and 2080s against PCIC's data of the baseline period 1974–2004 are presented as percentage over Fort Simpson and Arctic Red River stations, respectively (Fig. 4). As expected, the temperature is projected to increase between 2.5 °C and 5 °C in the 2050s, and between 3 °C and 8 °C in the 2080s at both Fort Simpson and Arctic Red River, respectively. The precipitation is projected to increase between 16% and 35% in the 2050s and between 18% and 43% in the 2080s at Arctic Red River. At Fort Simpson, the precipitation is projected to increase between 15% and 32% in the 2050s and between 15% and 40% in the 2080s. Both temperature and precipitation are projected to change over a relatively wide range under RCP8.5 scenarios in 2080s (see Fig. 4).

5.3. Water levels at Arctic Red River station

The streamflow regimes and water levels at the Arctic Red River based on downscaled climate scenarios of IPCC (2013) are presented as boxplots representing weekly streamflow over the historic period (1974–2004), and projected changes in 2050s and 2080s. As shown in Fig. 5a, water levels simulated from driving HBV with ANUSPLIN data over the historical period show a generally similar range than the observed streamflow in the summer. The peak streamflow in the spring (April and May) simulated is lower, and the winter base flow simulated are marginally lower than the observed, which is expected partly because of the flow regulation by the W.A.C. Bennet Dam. On the other hand, over 1974–2004, HBV driven by PCIC's statistically downscaled data simulated a marginally earlier spring melt (between the 14th and the 20th weeks). Historically the navigation season on the Mackenzie River is from June to October on average. Between June and October the mean water level simulated by HBV using GCMs' data correspond well to the mean observed water levels over 1974–2004 (Fig. 5b).

To present the average projected change at the Arctic Red station, the average projected hydrograph of HBV driven by RCP4.5 and RCP8.5 climate scenarios of each GCM are shown in Fig. 5c and d expressed in water levels. Average water levels based on HBV's simulations for both RCP4.5 and RCP8.5 climate scenarios generally show a lower peak in the summer, an earlier spring snowmelt, and a higher winter base flow compared to the historical period. Water levels are consistently projected to be higher than the observed during spring (April and May), but generally at the expense of lower than observed summer water levels for all climate scenarios considered in both periods. This is because of more rainfall and less snowfall, an earlier onset of spring snowmelt and more evaporation loss in the summer under a warmer climate in the future (See Section 3.6 and 3.7). The winter base flow simulated are marginally lower than the observed, which is partly because of the flow regulation by the W.A.C. Bennet Dam.

Compared to the historic period, the peak summer water level is projected to be on average about 1 m lower, and the water level is projected to remain lower throughout the summer of 2050s (Fig. 5c). Similar changes are projected for the 2080s (Fig. 5d), and the spring snowmelt could occur up to 4 weeks earlier than the observed. The peak flow could occur on an average by about a week earlier than the historic period, but the summer water levels projected at the Arctic Red between June and October based on downscaled climate scenarios of ACCESS1, CCSM4, CNRM-CM5, CSIRO-MK3-6, inmcm4, and MPI-ESM-LR are about 0.5 to 1.5 m lower than observed summer water levels (Fig. 5d).

For all climate scenarios of ten GCMs considered, the projected summer water levels vary widely, up to a difference of 1.5 m between the lowest (MPI-ESM-LR) and the highest (MRI-CGCM3) projected summer water levels. Between these two GCMs, the difference in the projected water levels based on RCP8.5 is larger than that based on RCP4.5 (Fig. 6a–d). Coincidentally, projected water levels in the 2050s under RCP8.5 are generally comparable to projected water levels in the 2080s under RCP4.5 (Fig. 6b and c). Most projected summer water levels are lower than the mean observed summer water levels. The difference between observed and projected summer water levels is mostly higher under RCP8.5 than RCP4.5 and in the 2080s than in the 2050s. There is generally a greater difference between projected water levels for the 2050s and the base period, than projected water levels between 2050s and 2080s (Fig. 6e). Fig. 6a–d show the range of possible streamflow diverges as we project into the distant future because differences between long-term climate projections of GCMs grow as we project towards the end of the 21st century, e.g., from about 1–2 m or less in 2050s to over 2 m in 2080s under RCP8.5. In other words, as expected uncertainties associated with projected water levels grow from 2050s to 2080s.

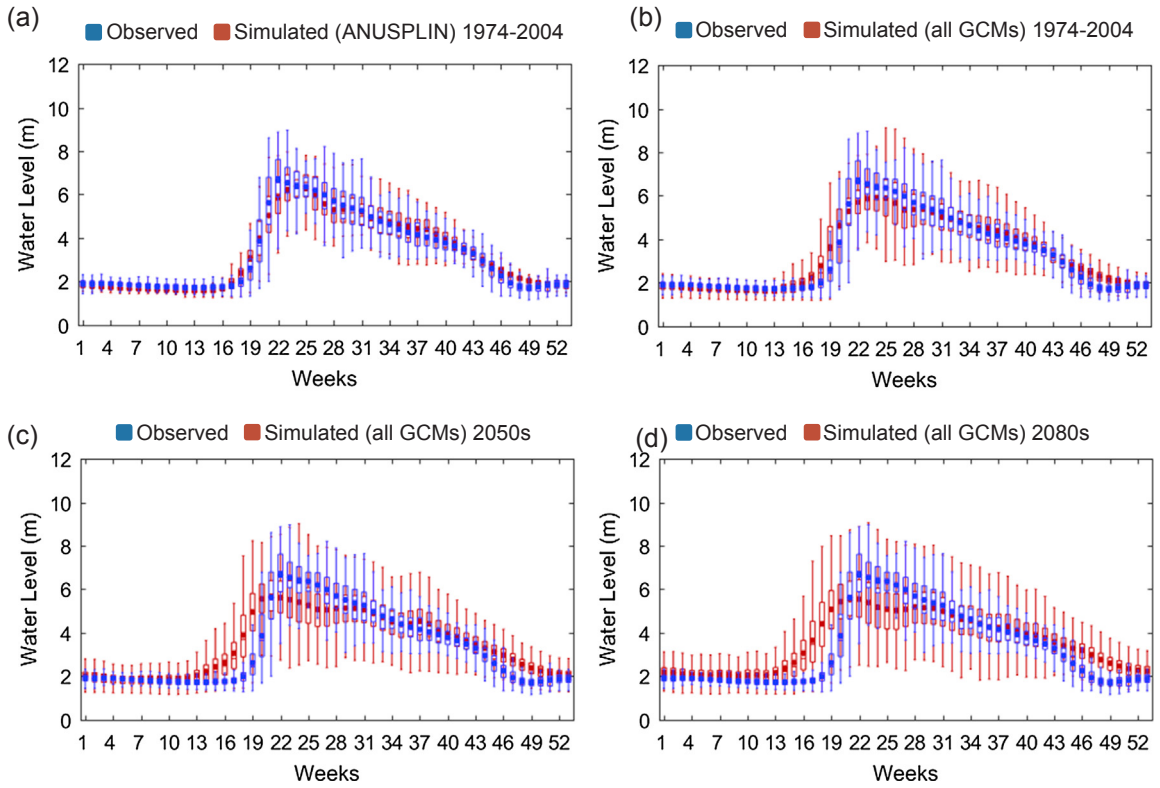

Fig. 5. Boxplots of Arctic Red River daily water levels observed between 1974 and 2004 plotted at weekly time steps versus the HBV's simulated water levels based on a) the ANUSPLIN data; b) GCMs' data for the baseline period 1974–2004; c) downscaled GCMs' climate scenarios under RCP 4.5 and RCP 8.5 for the 2050s; d) downscaled GCMs' climate scenarios under RCP 4.5 and RCP 8.5 for the 2080s. (For interpretation of the references to colour in this figure legend, the reader is referred to the web version of this article.)

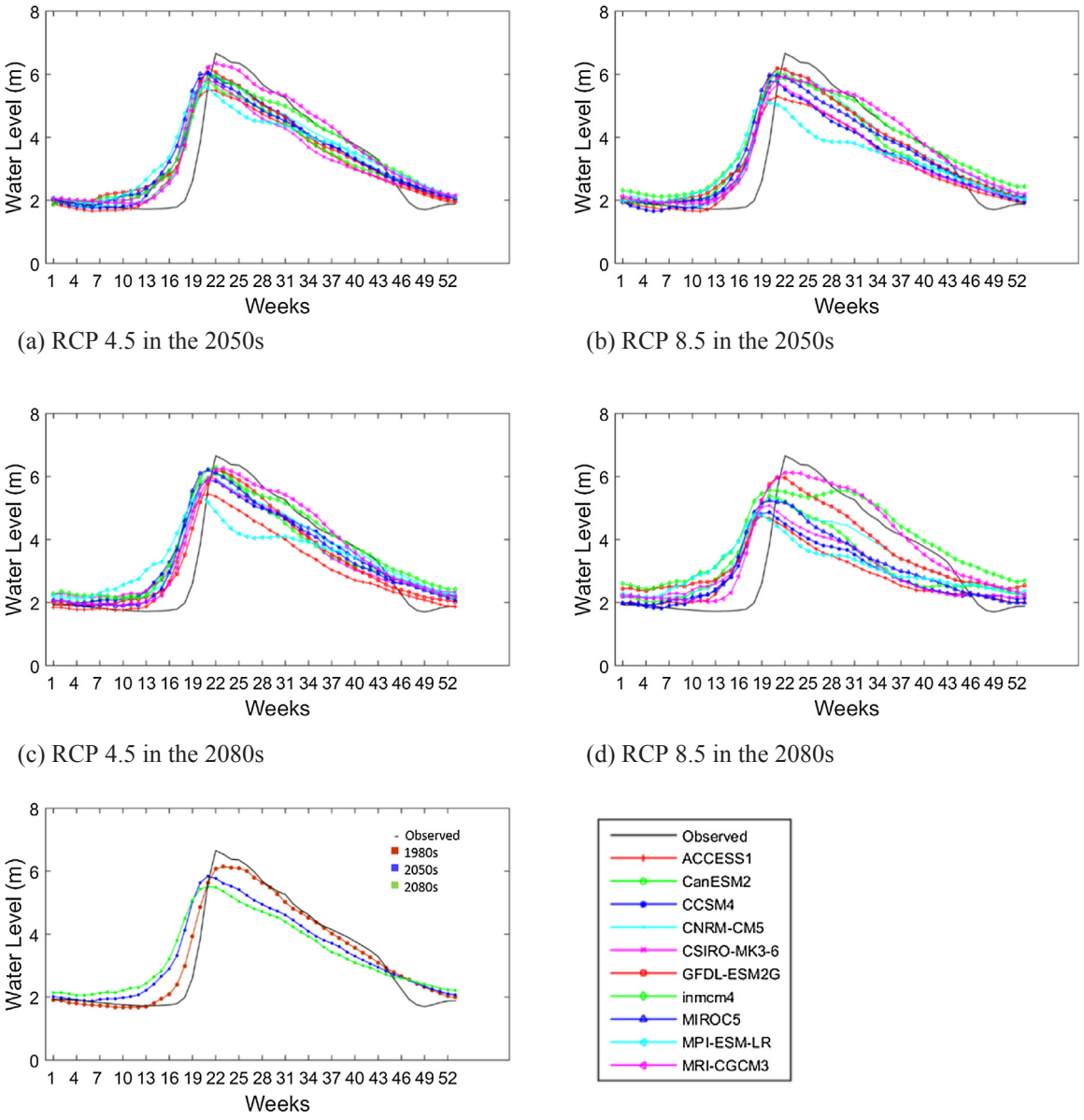

Fig. 6. Projected weekly water levels at Arctic Red River under a) RCP 4.5 climate scenarios in the 2050s; b) RCP 8.5 climate scenarios in the 2050s; c) RCP 4.5 climate scenarios in the 2080s; d) RCP 8.5 climate scenarios in the 2080s; and e) Mean water levels observed in the base period 1974–2004 and the projected in the 2050s and 2080s. (For interpretation of the references to colour in this figure legend, the reader is referred to the web version of this article.)

5.4. Water levels at Fort Simpson River station

Annual hydrographs simulated by HBV expressed as weekly water levels at Fort Simpson are shown in Fig. 7. Water levels simulated at Fort Simpson generally agree with the observed water levels, even though it marginally simulated higher water levels between August and October (Fig. 7e). HBV also marginally over-simulated the spring snowmelt streamflow in April and May, but it is closer to the observed at Fort Simpson than at Arctic Red River stations. The marginal discrepancies could be caused by either the limitations of HBV or the accuracy of the climate data. Over the same historic period, streamflow simulated by HBV driven by the 10 sets of statistically downscaled GCMs' climate data show higher simulated water levels between March and April, but between June and October the mean simulated water levels using the GCMs' data agree well with mean observed water levels (Fig. 7e). HBV simulated a wide range of possible water levels for 1974–2004 compared to the historical observations, especially during the peak flow period. Overall, HBV simulated water levels over the base period that are generally comparable to the historical observations, except during the spring snowmelt period and towards the end of summer.

HBV driven by GCMs' RCP4.5 and RCP8.5 climate scenarios in the 2050s and the 2080s simulated a wide range of water levels at Fort Simpson (Fig. 7), which exceed the range of water levels simulated by HBV further downstream at the Arctic Red River station. As expected, under the impact of climate change, HBV simulated an earlier onset of spring melt, lower peak water levels and lower summer water levels at both the Fort Simpson and the Arctic Red River stations.

5.5. Annual and seasonal water volume

It appears that under RCP climate scenarios of IPCC (2013) studied herein, a shift to earlier spring freshets but lower summer flows are projected for the future navigational spring and summer seasons of

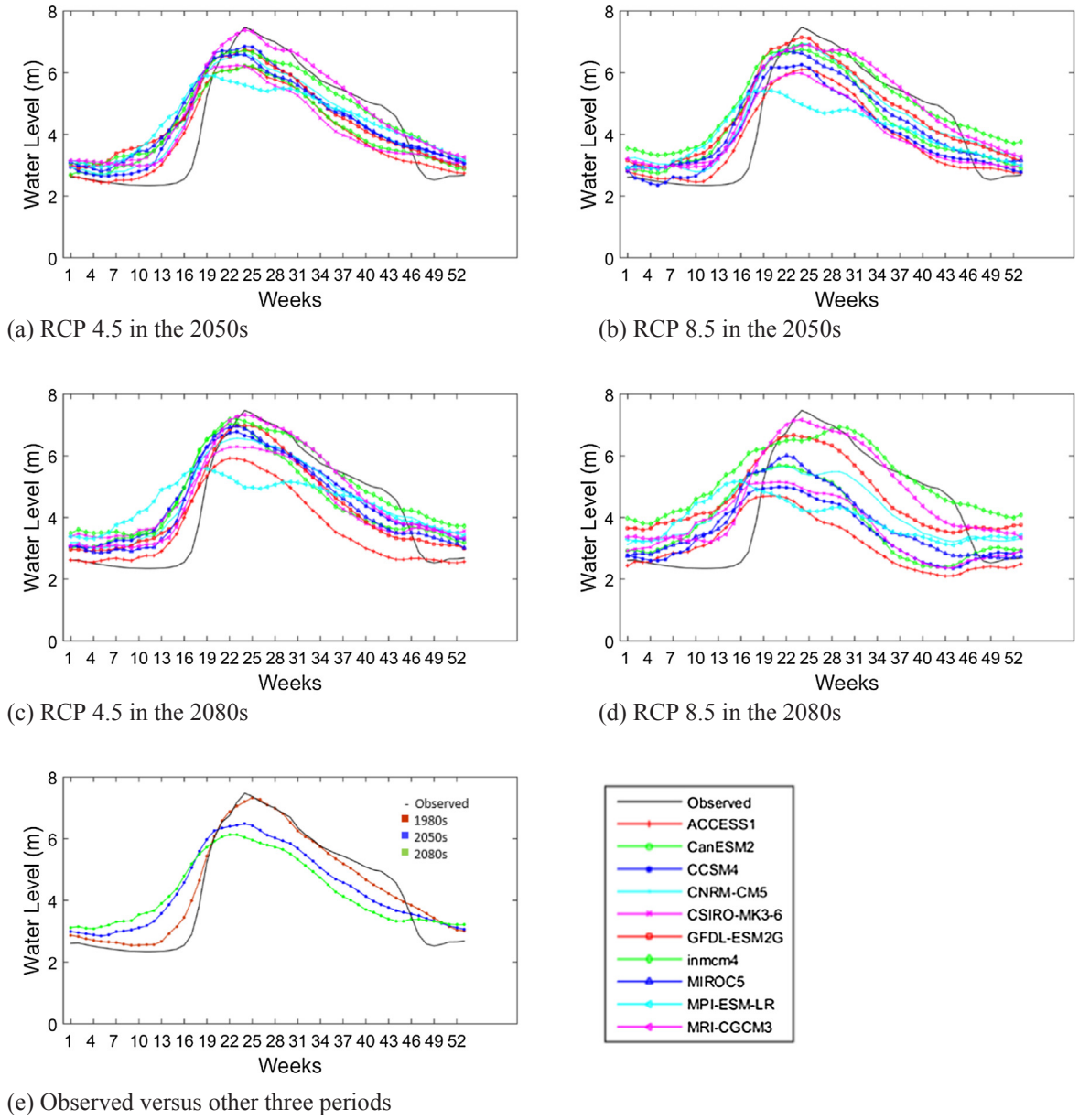

Fig. 7. Projected weekly water levels at Fort Simpson under a) RCP 4.5 climate scenarios in the 2050s; b) RCP 8.5 climate scenarios in the 2050s; c) RCP 4.5 climate scenarios in the 2080s; d) RCP 8.5 climate scenarios in the 2080s; and e) Mean water levels observed in the base period 1974–2004 and the projected in the 2050s and 2080s.

MRB. The average annual streamflow over 1974–2004 at Fort Simpson and Arctic Red River was 227.2 km^3 and 292.3 km^3, respectively (Table 5). The average annual streamflow is projected to decrease marginally from 1.4% to 6.4% under most climate scenarios, but it could decrease by 15.0% at Fort Simpson in the 2080s under RCP8.5, and marginally increase by 1.0% at Arctic Red River in the 2080s under RCP4.5. However, the average summer streamflow under all RCP climate scenarios considered is projected to decrease over 10% at Fort Simpson, but up to 30.4% under RCP8.5 in the 2080s. A similar change is projected for the Arctic Red River station where its streamflow is projected to decrease by 20.3% under RCP8.5 in the 2080s and about 6.5% to 8.5% under RCP4.5 in both periods and under RCP8.5 in the 2050s. In contrast, the average winter streamflow under all climate scenarios considered is projected to increase from 14.8% to 37.7% in both periods.

Overall, above results suggest that because of climate change impact, the annual hydrograph is projected to shift; the total annual streamflow is expected to decrease, particularly the summer streamflow, which is projected to decrease more in 2080s than in 2050s at both Fort Simpson and Arctic Red River stations. However, under a warmer climate, the winter streamflow is projected to increase in the 2050s and even more in the 2080s at both stations. Overall, the future streamflow of MRB is projected to increase in the winter at the expense of the summer.

5.6. Snow water equivalent

Spring snowmelt is a major source of water for MRB. The average annual SWE (snow water equivalent) at Fort Simpson is projected to decrease by about 15.2% and 21.3% in the 2050s and 2080s under RCP4.5, and to decrease by about 17% and 41% in the 2050s and 2080s under RCP8.5, respectively (Fig. 8). The average annual SWE at Arctic Red River is projected to decrease by about 5.5% and 6.2% under RCP4.5 in the 2050s and 2080s, and 9.2% and 20.1% in the 2050s and

Table 5
Projected changes to the annual, summer (May to October), and winter (November to April) discharge in km^3 and in percentage (%), and the days during May to October above or at different water levels, at Fort Simpson and Arctic Red River stations under all RCP climate scenarios considered for both periods.

Discharge (km^3) and Changes in %	Fort Simpson					Arctic Red River				
	Historical simulations	RCP 4.5		RCP 8.5		Historical simulations	RCP 4.5		RCP 8.5	
	1974–2004	2050s	2080s	2050s	2080s	1974–2004	2050s	2080s	2050s	2080s
Annual	227.2	216.0 (−5.0%)	222.0 (−2.3%)	213.3 (−6.1%)	193.1 (−15.0%)	292.3	288.2 (−1.4%)	295.4 (1.0%)	286.8 (−1.9%)	273.6 (−6.4%)
Summer	163.6	142.5 (−12.9%)	144.8 (−11.5%)	140.2 (−14.3%)	113.9 (−30.4%)	222.3	205.8 (−7.4%)	207.7 (−6.5%)	203.3 (−8.5%)	177.2 (−20.3%)
Winter	63.6	73.4 (15.4%)	77.2 (21.3%)	73.0 (14.8%)	79.2 (24.6%)	70.1	82.4 (17.6%)	87.6 (25.1%)	83.5 (19.2%)	96.4 (37.7%)
Water Levels (m)	Days during May to October above or at different water levels (Changes in %)									
3	181	176 (−2.8%)	173 (−4.4%)	170 (−6.1%)	145 (−19.9%)	167	159 (−4.8%)	156 (−6.6%)	154 (−7.8%)	130 (–22.2%)
4	168	150 (−10.7%)	147 (−12.5%)	143 (−14.9%)	110 (−34.5%)	120	108 (−10.0%)	108 (−10.0%)	104 (−13.3%)	81 (–32.5%)
5	129	106 (−17.8%)	107 (−17.1%)	104 (−19.4%)	73 (−43.4%)	74	60 (−18.9%)	62 (−16.2%)	58 (−21.6%)	42 (−43.2%)

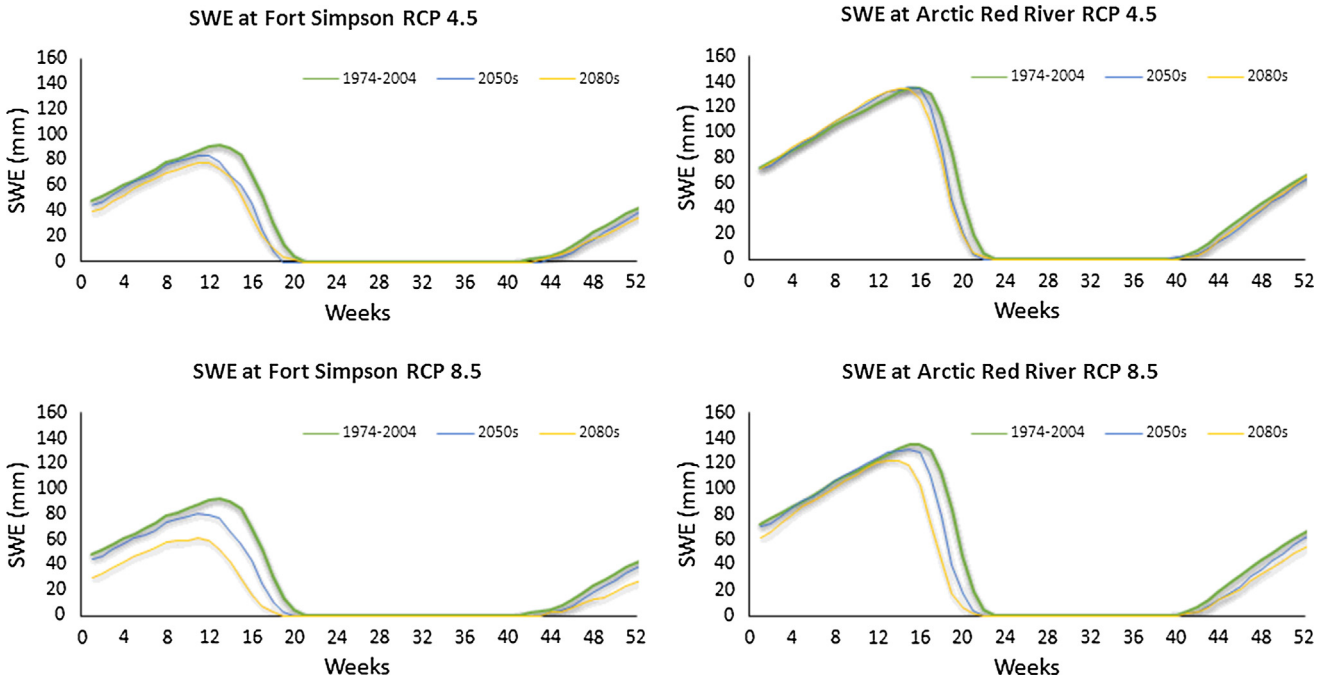

Fig. 8. Projected snow water equivalent (SWE) at Fort Simpson and Arctic Red River, under RCP 4.5 climate scenarios in the 2050s; RCP 8.5 climate scenarios in the 2050s; RCP 4.5 climate scenarios in the 2080s; RCP 8.5 climate scenarios in the 2080s; and in the base period 1974–2004. (For interpretation of the references to colour in this figure legend, the reader is referred to the web version of this article.)

2080s under RCP8.5, respectively, which are less compared to Fort Simpson probably because of its higher latitude location. Even though the winter precipitation at Fort Simpson is projected to increase by 27.6% under RCP8.5, and the winter water levels, its SWE is projected to decrease substantially in the 2080s. Decreasing SWE trends are partly related to the tendency of an earlier onset of spring melt, and more precipitation during winter will occur as rainfall instead of snowfall under a warmer climate, which would increase the winter streamflow as shown in previous sections. Decreasing SWE trends in North America have been detected from passive microwave data collected between 1979 and 2007 (Gan et al., 2013). As expected, projected decrease in SWE would affect the hydrology of MRB, particularly resulting in less summer streamflow.

5.7. Evapotranspiration

The amount of actual evapotranspiration (AET) simulated by HBV depends on the soil moisture and the potential evapotranspiration. Under RCP climate scenarios, the warm period is expected to begin in late March and to continue to early November. Similarly, evapotranspiration will begin in late March, peaks in July and declines until November at both stations (Fig. 9). The annual total AET is projected to increase under all RCP climate scenarios and in both periods, particularly under RCP8.5 and in the 2080s, which is partly why the summer streamflow is consistently projected to decrease from 2050s to 2080s. Although the annual distribution of AET may only change marginally, the projected increase in the annual total evapotranspiration of MRB is relatively large, 13.7%–34.0%, compared with the projected increase of 10.3%–26.2% in the mean annual precipitation, which resulted in less total streamflow, especially the summer.

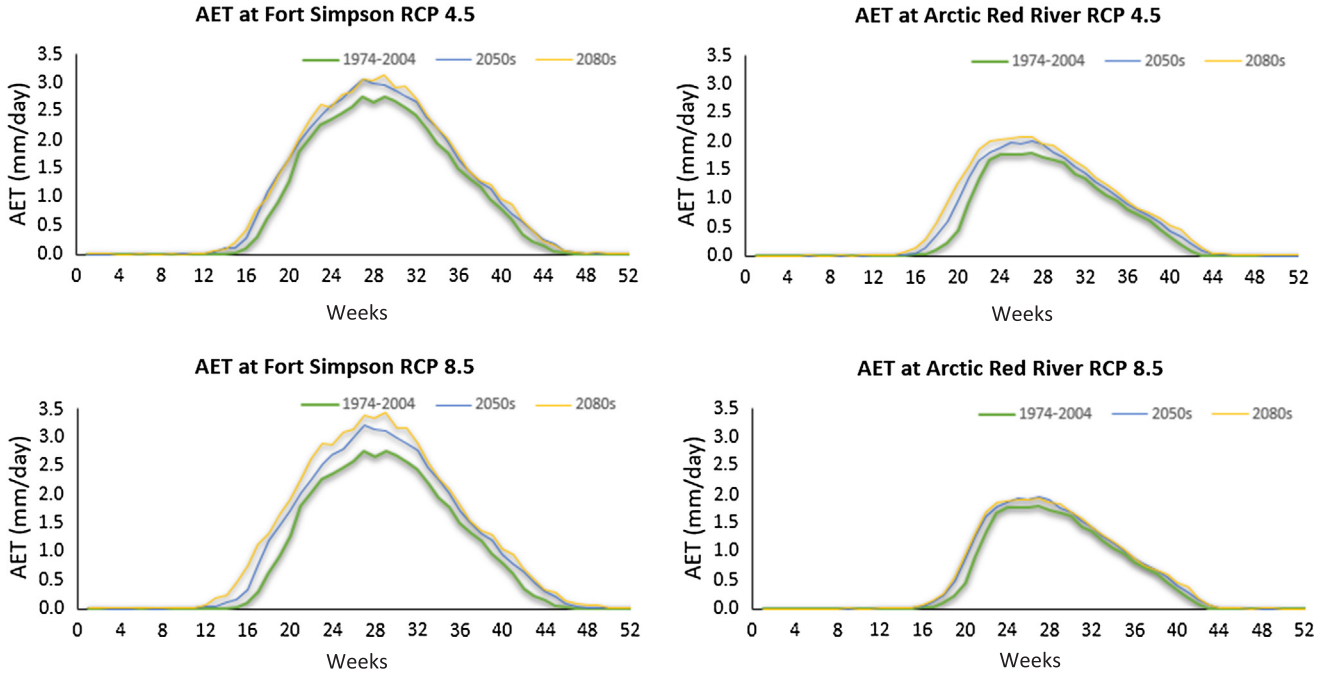

Fig. 9. Projected increase in the actual evapotranspiration (AET) at Fort Simpson and Arctic Red River under RCP 4.5 climate scenarios in the 2050s; RCP 8.5 climate scenarios in the 2050s; RCP 4.5 climate scenarios in the 2080s; RCP 8.5 climate scenarios in the 2080s; and in the base period 1974–2004. (For interpretation of the references to colour in this figure legend, the reader is referred to the web version of this article.)

5.8. Days above or at different water levels from May to October

In high latitudes, the presence of river ice limits shipping in the Mackenzie River to a short summer ice-free season, which also depends on water levels and weather conditions. The depth that a vessel will sink into the water depends on its load. For a heavy load, the depth will be greater, and therefore the goods carrying capacity of a barge is directly affected by the water level of the river. Typically, the shipping season of the Mackenzie River is from May to October. Even though a warmer climate will lead to an earlier ice breakup in spring and later freezing in autumn, in this study we chose to investigate possible changes to water levels from May to October because it has been the Arctic shipping season. The average number of days that water levels exceed certain thresholds between May to October under different climate change scenarios will directly affect the shipping schedule and transportation problems in the Arctic. Changes in the timing of low water levels can also affect the northern navigation and projected reduction in water levels will incur negative impacts to commercial shipping operations in the Mackenzie River (Zheng and Kim, 2017).

At Fort Simpson and Arctic Red River stations, the number of days that water levels will be above 3 m and 4 m are projected to decrease in the 2050s and more severely in the 2080s, while the number of days that water levels above 5 m are projected to decrease marginally more in the 2080s than in the 2050s under RCP4.5 and RCP8.5, respectively (see Table 5 which shows ensemble mean water levels). At Fort Simpson, the number of days that water levels will be above 5 m under RCP4.5 (RCP8.5) is projected to decrease by 17.8 (19.4)% in the 2050s and 17.1 (43.4)% in the 2080s. They are projected to decrease by −18.9 (21.6) % in the 2050s and 16.2 (43.2) % in the 2080s at the Arctic Red River station. For water levels above 3 m, under RCP4.5 (RCP8.5), the numbers of days are projected to decrease by 2.8 (6.1) % and 4.8 (7.8) % in the 2050s, and 4.4 (19.9)% and 6.6 (22.2)% in the 2080s for Fort Simpson and Arctic Red River stations, respectively. Under RCP8.5, the number of days that water levels will be above 3 m is expected to decrease by 36 days at Fort Simpson in the 2080s. At the downstream Arctic Red River Station, the number of days the water level is projected to be lower than 3–5 m are expected to be less than at Fort Simpson, which could affect the shipping operation further north. The average duration of the navigation season under RCP4.5 (RCP8.5) with a water level of 5 m or higher in the 2080s has been estimated to be 107 (73) days and 62 (42) days for the Fort Simpson and Arctic Red River stations, respectively. Therefore, under the potential impact of climate change, especially under RCP8.5, navigation problems are expected to get worse in the 21st Century because a safe transit through the Mackenzie River depends on its water levels.

6. Summary and conclusions

The potential impact of climate change on the water levels of the Mackenzie River was investigated by forcing the conceptual hydrological model, HBV-light, at five locations within the MRB with RCP4.5 and RCP8.5 climate scenarios of ten GCMs statistically downscaled by PCIC using the BCSD method. The analyses included temperature, precipitation, streamflow, water levels, discharge volume, SWE, the actual evapotranspiration, and the number of days that water levels are above certain thresholds. The time periods considered were the historic period, 1974–2004, and the projected periods, 2050s (2041–2070) and 2080s (2071–2100).

Under RCP4.5 climate scenarios, the air temperature (precipitation) of MRB is projected to increase by 2.3–2.5 °C (6.4–9.5%) in the 2050s and 2.7–3.1 °C (10.7–12.1%) in the 2080s. Under RCP8.5 climate scenarios, the air temperature (precipitation) of MRB is projected to increase by 2.8–3.1 °C (9.8–13.2%) and 4.8–5.4 °C (16.1–21.0%) in the 2050s and 2080s, respectively. In other words, RCP8.5 climate scenarios project a larger change in precipitation than RCP4.5 in 2050s and 2080s. Based on results obtained from RCP climate scenarios, temperature and precipitation are generally projected to increase to a larger extent in northern than in southern sub-basins of MRB.

Driven with gridded ANUSPLIN data, the HBV-light model was calibrated and validated independently against observed streamflow of Fort Simpson and Arctic Red River stations. At the calibration and validation stages, R^2 (Nash-Sutcliffe coefficient, NS) obtained at Fort Simpson are 0.89 and 0.85 (0.88 and 0.74), respectively. The corresponding R^2 (NS) obtained for the Arctic Red River station are 0.89 and

0.87 (0.88 and 0.73), respectively. Under downscaled RCP4.5 and RCP8.5 climate scenarios of 10 GCMs of IPCC (2013), the streamflow and water level of the Mackenzie River at Fort Simpson and Arctic Red River stations are projected to increase in winter and spring but at the expense of the summer streamflow and water level, because the projected increase in evapotranspiration loss offset the projected increase in precipitation in the summer, and SWE is projected to decrease because more rainfall and less snowfall under warmer climate. The spring streamflow and water levels are projected to increase because warming will result in an earlier onset of spring snowmelt in MRB.

Given the projected, earlier spring snowmelt but reduced water levels in the summer, climate change is expected to affect the Arctic ferry operations of the Mackenzie River, which could start earlier because a warmer climate will cause an earlier onset of spring snowmelt and higher spring discharge. Under RCP8.5 scenarios, the number of days the water level at Arctic Red River station will be above 5 m is projected to decrease from 74 in 1974–2000 to only 42 days in the 2080s. The total duration that water levels of the Mackenzie River at Fort Simpson and Arctic Red River stations will be above or at 3 m, 4 m, 5 m are expected to decrease by 2.8%–22.2%, 10.0%–34.5%, 16.2%–43.4%, respectively. Given the summer water levels of the Mackenzie are projected to decrease in the 2050s and 2080s, navigation problems related to low water levels are expected to increase because safe transit through the Mackenzie River depends on its water levels.

Because statistical downscaling approaches have limitations in projecting GCMs' climate scenarios to a future climate as the climate data they are trained on is not necessarily the same as what the future will be, an extension of this study is to use RCMs to dynamically downscale RCP climate scenarios of GCMs of IPCC. Kuo and Gan (2018) have set up and fine-tuned a RCM, Weather Research Forecasting (WRF), to downscale RCP climate scenarios of limited number of GCMs, given dynamic downscaling is computationally intensive and time consuming (e.g., Hanrahan et al., 2014). A hydrological model will similarly be forced with downscaled RCP climate scenarios of WRF to assess the impact of climate change to the Mackenzie River Basin.

Acknowledgements

This study was funded by the Transport Canada under its Northern Transport Adaptation Initiative program, and partly by the Natural Science and Engineering Research Council of Canada. The ANUSPLIN, HYDAT, climate station data, and PCIC statistically downscaled RCP climate scenarios, were downloaded from the websites of Environment Canada and PCIC of University of Victoria, respectively. The hydrologic model, HBV, was provided by Dr. Seibert of University of Zurich, Switzerland.

References

Arctic Council (2009) Arctic Marine Shipping Assessment, 2009 Report, pp. 194.
Barry, R., Gan, T.Y., 2011. Global Cryosphere, Past, Present and Future. Cambridge University Press, pp. 472 ISBN: 9780521769815.
Bergstrom, S., 1975. The development of a snow routine for the HBV-2 model. Nordic Hydrol. 6 (2), 73–92.
Bergstrom, S., Carlsson, B., Gardelin, M., Lindstrom, G., Pettersson, A., Rummukainen, M., 2001. Climate change impacts on runoff in Sweden – assessments by global climate models, dynamical downscaling and hydrological modelling. Climate Res. 16, 101–112.
Cohen, S.J. (1997) Mackenzie Basin Impact Study. Final Report. Ottawa, Ontario, CN: Environment Canada.
Environment Canada (2013) HYDAT Database. Available from: https://www.ec.gc.ca/rhcwsc/default.asp?lang=En&n=9018B5EC-1, Water Survey of Canada.
Environment and Natural Resources, GNWT (2008) Environment & Natural Resources, GNWT NWT Climate Change Impacts and Adaptation Report.
Gan, T.Y., Mari Ito, S., Huelsmann, X Qin, Lu, X., Liong, S.Y., Rutschman, P., Disse, M., Koivosalo, H., 2016. Possible climate change/variability and human impacts, vulnerability of African drought prone regions, its water resources and capacity building. Hydrol. Sci. J. https://doi.org/10.1080/02626667.2015.1057143.
Gan, T.Y., Barry, R., Gobena, A., Rajagopalan, B., 2013. Changes in North America Snowpacks for 1979–2007 detected from the snow water equivalent data of SMMR and SSM/I passive microwave & related climatic factors. J. Geophysic. Research-Atm. 118 (14), 7682–7697. https://doi.org/10.1002/jgrd.50507.
Gobena, A., Gan, T.Y., 2013. Assessment of trends and possible climate change impacts on summer moisture availability in western canada based on metrics of the palmer drought severity index. J. Clim., AMS 26 (13), 4583–4595. https://doi.org/10.1175/JCLI-D-12-00421.1.
Hamon, W.R., 1961. Estimating potential evapotranspiration. J. Hydraul. Divis. Proceed. Am. Soc. Civ. Eng. 87 (HY3), 107–120.
Hanrahan, J., Kuo, C.C., Gan, T.Y., 2014. Configuration and validation of a mesoscale atmospheric model for simulating summer rainfall in Alberta. Int. J. Climatol. RMS 35 (5), 660–675. https://doi.org/10.1002/joc.4011.
Hicks, F.E., Steffler, P.M., 1992. Characteristic dissipative galerkin scheme for open-channel flow. J. Hydraul. Eng.-Asce 118, 337–352.
Huntington, H., Fox, S., 2005. The changing Arctic: indigenous perspectives. In: Arctic Climate Impact Assessment. Cambridge University Press, Cambridge, UK, pp. 61–98.
Hutchinson, M.F., Mckenney, D.W., Lawrence, K., Pedlar, J.H., Hopkinson, R.F., Milewska, E., Papadopol, P., 2009. Development and testing of Canada-wide interpolated spatial models of daily minimum-maximum temperature and precipitation for 1961–2003. J. Appl. Meteorol. Clim. 48, 725–741.
IPCC, 2007. Climate Change 2007: The Physical Science Basis. Contribution of Working Group I to the Fourth Assessment Report of the Intergovernmental Panel on Climate Change. Cambridge University Press, Cambridge, United Kingdom and New York, NY, USA.
IPCC, 2014. Climate Change 2014: Mitigation of Climate Change. Contribution of Working Group III to the Fifth Assessment Report of the Intergovernmental Panel on Climate Change. Cambridge University Press, Cambridge, United Kingdom and New York, NY, USA.
IPCC Fifth Assessment Report: Working Group I (WGI) report, 2013. Intergovernmental panel on climate change. Available from. http://www.ipcc.ch/.
Jiang, R.G., Gan, T.Y., Xie, J., Ni, W., 2014. Spatiotemporal variability of Alberta's seasonal precipitation, their teleconnection with large-scale climate anomalies and sea surface temperature. Int. J. Climatol. RMS 34 (9), 2899–2917. https://doi.org/10.1002/joc.3883.
Kendall, M.G., 1948. Rank Correlation Methods. C. Griffin, London.
Kerr, J.A. 1997. Future water levels and flows for Great Slave and Great Bear Lakes, Mackenzie River, and Mackenzie delta. In: Cohen, S.J., ed. Mackenzie Basin Impact Study Final Report. Downsview, Ontario: Environment Canada. 73-91.
Kouwen, N., Soulis, E.D., Pietroniro, A., Donald, J., Harrington, R.A., 1993. Grouped Response Units for Distributed Hydrologic Modeling. J. Water Res Pl. ASCE 119, 289–305.
Kuo, C.C., Gan, T.Y., 2018. Estimation of precipitation and air temperature using WRF over Mackenzie River Basin. Interna. J. Climatology 2018, 1–11. https://doi.org/10.1002/joc.5716.
Kuo, C.C., Gan, T.Y., Higuchi, K., 2017. Potential impacts of climate change to streamflow patterns of River basins of Lake Simcoe. J. Hydrol. Eng. 22 (9), 04017028. https://doi.org/10.1061/(ASCE)HE.1943-5584.0001548.
Kuo, C.C., Gan, T.Y., Gizaw, M., 2015. Potential impact of climate change on intensity duration frequency curves of central Alberta. Climatic Change 130, 115–129. https://doi.org/10.1007/s10584-015-1347-9.
Land Processes Distributed Active Archive Center (LP DAAC), (2012) Land Cover Type Yearly L3 Global 500 m SIN Grid. MCD12Q1 version V051. NASA EOSDIS Land Processes DAAC, USGS Earth Resources Observation and Science (EROS) Center, Sioux Falls, South Dakota, accessed 1/23/2015, https://lpdaac.usgs.gov/dataset_discovery/modis/modis_products_table/mcd12q1].
Mann, H.B., 1945. Nonparametric tests against trend. Econometrica. J. Economet. Soc. 245–259.
Maurer, E.P., Hidalgo, H.G., 2008. Utility of daily vs. monthly large-scale climate data: an intercomparison of two statistical downscaling methods. Hydrol. Earth Syst. Sci. 12, 551–563.
McKinnon A. 2007. CO2 emissions from freight transport: an analysis of UK data. In Logistics Research Network-2007, Conference Global Supply Chains: Developing Skills, Capabilities and Networks.
Mekis, É., Vincent, L.A., 2011. An overview of the second generation adjusted daily precipitation dataset for trend analysis in Canada. Atmosphere-Ocean 49 (2), 163–177.
Mwale, D., Gan, T.Y., Devito, K., Silins,, 2009. Precipitation variability & its relationship to hydrologic variability and physical features in Alberta. Hydrol. Proc. 23 (21), 3040–3056. https://doi.org/10.1002/hyp.7415.
Nash, J.E., Sutcliffe, J.V., 1970. River flow forecasting through conceptual models part I – A discussion of principles. J. Hydrol. 10 (3), 282–290.
Press, W.H., Teukolsk, S.A., Vetterling, W.T., Flannery, B.P., 2002. Numerical recipes in C++: the art of scientific computing, Second ed. Cambridge University Press, Cambridge, UK.
Seibert, J., Vis, M.J.P., 2012. Teaching hydrological modeling with a user-friendly catchment runoff-model software package. Hydrol. Earth Syst. Sc. 16, 3315–3325.
Seibert, J., 2000. Multi-criteria calibration of a conceptual runoff model using a genetic algorithm. Hydrol. Earth Syst. Sc. 4, 215–224.
Sen, P.K., 1968. Estimates of the regression coefficient based on Kendall's tau. J. Am. Statist. Assoc. 63 (324), 1379–1389.
Seneka, M., 2004. Trends in historical annual flow for major rivers in Alberta. Tec. Rept., Alberta.
Soulis, E, Solomon S, Lee M., Kouwen N (1994) Changes to the distribution of monthly and annual runoff in the Mackenzie Basin using a modified square grid approach. in Cohen SJ (ed.), Mackenzie Basin Impact Study, Interim Report #2, Proc. of 6th Biennial AES/DIAND Meeting on Northern Climate and Mid Study Workshop of MBIS, Yellowknife, NWT, April 10-14, Environment Canada, Downsview, pp. 197–209.

Singh, P.R., Gan, T.Y., Gobena, A.K., 2009. Evaluating a hierarchy of snowmelt models at a watershed in the Canadian Prairies. J. Geophys. Res. 114, D04109. https://doi.org/10.1029/2008JD010597.

Stewart, R.E., Leighton, H.G., Marsh, P., Moore, G.W.K., Ritchie, H., Rouse, W.R., Soulis, E.D., Strong, G.S., Crawford, R.W., Kochtubajda, B., 1998. The Mackenzie GEWEX Study: The water and energy cycles of a major North American river basin. B. Am. Meteorol. Soc. 79, 2665–2683.

Sung, R.Y.J., Burn, D.H., Soulis, E.D., 2006. A case study of climate change impacts on navigation on the Mackenzie River. Canad. Water Resour. J. 31 (1) 68–57.

Takala, M., Luojus, K., Pulliainen, J., Derksen, C., Lemmetyinen, J., Kärnä, J., Koskinen, J., Bojkov, B., 2011. Estimating northern hemisphere snow water equivalent for climate research through assimilation of space-borne radiometer data and ground-based measurements. Remote Sens. Environ. 115 (12), 3517–3529.

Theil, H., 1950. A rank-invariant method of linear and polynomial regression analysis, 1,2, and 3. Ned. Akad. Wentsch Proc. 53 386–392, 521–525, and 1397–1412.

Trenberth, K.E., Dai, A., Rasmussen, R.M., Parsons, D.B., 2003. The changing character of precipitation. B. Am. Meteorol. Soc. 84, 1205–1217.

Vehviläinen, B., Huttunen, M., 1997. Climate change and water resources in Finland. Boreal. Env. Res. 2 (1), 3–18.

Vincent, L.A., Wang, X.L., Milewska, E.J., Wan, H., Yang, F., Swail, V., 2012. A second generation of homogenized Canadian monthly surface air temperature for climate trend analysis. J. Geophys. Res. 117, D18110. https://doi.org/10.1029/2012JD017859.

Weller, G., et al., 2005. Summary and synthesis of the ACIA. In: Arctic Climate Impact Assessment. Cambridge University Press, Cambridge, UK, pp. 989–1020.

Werner, A.T. 2011. BCSD Downscaled Transient Climate Projections for Eight Select GCMs over British Columbia, Canada. Pacific Climate Impacts Consortium, Uni. of Victoria, BC, pp. 63.

Werner, A.T., Cannon, A.J., 2015. Hydrologic extremes – an intercomparison of multiple gridded statistical downscaling methods. Hydrol. Earth Syst. Sci. Discuss. 12, 6179–6239. https://doi.org/10.5194/hessd-12-6179-2015.

Werner, A.T., Cannon, A.J., 2016. Hydrologic extremes – an intercomparison of multiple gridded statistical downscaling methods. Hydrol. Earth Syst. Sci. Discuss. 20, 1483–1508. https://doi.org/10.5194/hess-20-1483-2016.

Wood, A.W., Leung, L.R., Sridhar, V., Lettenmaier, D.P., 2004. Hydrologic implications of dynamical and statistical approaches to downscaling climate model outputs. Climatic Change 62, 189–216.

Zheng, Y., Kim, A., 2017. Rethinking business-as-usual: mackenzie river freight transport in the context of climate change impacts in Northern Canada. Transport. Res. Part D: Transport Environ. 53, 276–289.